

Temperature dependence of spatially heterogeneous dynamics in a model of viscous silica

Michael Vogel* and Sharon C. Glotzer†

*Department of Chemical Engineering and Department of Materials Science and Engineering,
University of Michigan, 2300 Hayward, Ann Arbor, MI, 48109, USA*

(Dated: November 10, 2018)

Molecular dynamics simulations are performed to study spatially heterogeneous dynamics in a model of viscous silica above and below the critical temperature of the mode coupling theory, T_{MCT} . Specifically, we follow the evolution of the dynamic heterogeneity as the temperature dependence of the transport coefficients shows a crossover from non-Arrhenius to Arrhenius behavior when the melt is cooled. It is demonstrated that, on intermediate time scales, a small fraction of oxygen and silicon atoms are more mobile than expected from a Gaussian approximation. These highly mobile particles form transient clusters larger than that resulting from random statistics, indicating that dynamics are spatially heterogeneous. An analysis of the clusters reveals that the mean cluster size is maximum at times intermediate between ballistic and diffusive motion, and the maximum size increases with decreasing temperature. In particular, the growth of the clusters continues when the transport coefficients follow an Arrhenius law. These findings imply that the structural relaxation in silica cannot be understood as a statistical bond breaking process. Though the mean cluster sizes for silica are at the lower end of the spectrum of values reported in the literature, we find that spatially heterogeneous dynamics in strong and fragile glass formers are similar on a qualitative level. However, different from results for fragile liquids, we show that correlated particle motion along quasi one-dimensional, string-like paths is of little importance for the structural relaxation in this model of silica, suggesting that string-like motion is suppressed by the presence of covalent bonds. To study spatial correlations between highly immobile particles, we calculate a generalized susceptibility corresponding to the self part of a four-point time dependent density correlation function. We find that this generalized susceptibility is maximum on the time scale of the structural relaxation, where a strong increase of the peak height indicates a growing length of spatial correlations between highly immobile particles upon cooling. Characterizing the local structures of the most mobile and the most immobile particles, respectively, we show that high particle mobility is facilitated by, but not limited to, the vicinity of defects of the network structure.

PACS numbers: 66.30.Dn

I. INTRODUCTION

Applications of various experimental methods demonstrated that the structural relaxation of many supercooled liquids exhibits dynamic heterogeneities, i.e., it is possible to select a subset of particles that rotate or translate much farther or shorter distances than an average particle.^{1,2,3,4,5,6} However, the majority of experimental techniques do not provide information about the spatial arrangement of mobile and immobile particles, which plays a central role in several theories of the glass transition.^{7,8,9} Recently, results of multidimensional nuclear magnetic resonance experiments showed that dynamics in polymers¹⁰ and in organic low-molecular weight compounds^{11,12} are spatially heterogeneous. Particles within a physical region of these viscous liquids show an enhanced or diminished mobility compared to particles in a region a few nanometers away. Despite this progress, an experimental characterization of the time evolution of spatially heterogeneous dynamics (SHD) is still lacking. Further, detailed experimental studies of the dynamical behavior of strong liquids, like silica, are hampered by the high glass transition temperatures, T_g , of these materials. Nevertheless, based on the Arrhenius behavior observed at sufficiently low temperatures, it is often ar-

gued that the dynamics in silica melts can be understood as a statistical bond breaking process.

Molecular dynamics (MD) simulations of model glass-forming liquids provide direct access to spatial correlations of particle mobility. Due to the available computer power, present simulations are performed at temperatures near T_{MCT} , the critical temperature of the mode-coupling theory (MCT),¹³ where the structural relaxation typically occurs on the order of nanoseconds. In previous work, MD simulations were used to investigate dynamic heterogeneity in soft-sphere^{14,15,16} and hard-sphere systems,¹⁷ binary Lennard-Jones (BLJ) mixtures,^{18,19,20,21,22,23,24,25,26,27} the Dzugutov liquid,^{29,30,31} polymer melts^{32,33,34,35} and molecular liquids.^{36,37} These studies showed that highly mobile and highly immobile particles aggregate into clusters that are transient in nature.

Specifically, highly mobile particles both in simple liquids, such as BLJ mixtures²² and the Dzugutov liquid,³⁰ and in more complex systems, like polymer melts³⁴ and water,³⁷ form clusters that are largest at times intermediate between ballistic and diffusive motion. The size of these clusters grows strongly when the liquid is cooled and a divergence at $T \approx T_{MCT}$ was proposed.^{22,38} Within the clusters smaller groups of particles move in

strings, i.e., particles follow each other along quasi one-dimensional paths. This correlated motion on intermediate time scales, which is believed to facilitate structural relaxation,³⁸ appears to be universal as well, as it is found for a range of different model liquids.^{21,22,30,35} In addition, spatial correlations of highly immobile particles were studied based on a four-point time dependent density correlation function.^{24,25,26,27,28,39} For BLJ liquids, it was observed that the corresponding generalized susceptibility $\chi_4(\Delta t)$ exhibits a maximum that increases with decreasing temperature, indicating that there is a growing length of spatial correlations between particles localized in a time interval Δt .

All these studies were performed in temperature ranges where the evolution of the relaxation times shows pronounced deviations from Arrhenius behavior. In a recent MD simulation study,⁴⁰ we demonstrated that SHD exists not only in fragile liquids, but also in a model of silica, the paradigm of a strong liquid.⁴¹ Specifically, the most mobile particles were found to form clusters larger than predicted from random statistics, where the mean cluster size is maximum at times intermediate between ballistic and diffusive motion, as was observed for other model liquids. Further, we showed that the dynamic heterogeneities are short lived so that high particle mobility spreads throughout the sample on the time scale of the structural relaxation. In doing so, the probability for a previously immobile particle to become mobile is enhanced in the vicinity of another mobile particle, supporting the concept of dynamic facilitation, which is the cornerstone of a microscopic model of viscous liquids proposed recently by Garrahan and Chandler.^{8,9} Finally, our previous results suggest that, compared to other model liquids, string-like motion is less relevant for the structural relaxation of silica.

In view of these findings for fragile and strong liquids, one may ask how the transport coefficients of viscous liquids – in particular their temperature dependence – are related to the properties of SHD. Indeed, the decoupling of diffusivity and viscosity or structural relaxation time, indicating a breakdown of the classic Stokes-Einstein relation, has been rationalized in terms of SHD.^{5,24} Furthermore, a link between the diffusion coefficient D and the clusters of mobile particles was observed in simulation studies of water.³⁷ Specifically, it was reported that the mean cluster size is a measure of the mass of the cooperatively rearranging regions central to the Adam-Gibbs theory,⁷ which in turn allows one to describe the temperature dependence of D . This suggests that the behavior of the transport coefficients, which describe the long-time liquid dynamics, is determined by SHD at intermediate times. On the other hand, Garrahan and Chandler^{8,9} emphasize that spatiotemporal characteristics of mobility propagation are important to rationalize differences between various glass formers. In particular, they argue that mobility propagation carries a direction, the persistence length of which is larger for fragile than for strong glass formers.

Here, we continue our MD simulation study of SHD in the BKS model of viscous silica,⁴² which is commonly used to reproduce structural and dynamical properties of this strong liquid.^{43,44,45,46,47,48,49,50,51} In this way, we wish to obtain further insights into the relaxation dynamics of one of the most important glass formers, which are difficult to extract from experimental studies. It is well established that the transport coefficients of BKS silica show a crossover from a non-Arrhenius to an Arrhenius temperature dependence upon cooling,^{44,45,46,47,48} in agreement with experimental data.⁵² Saika-Voivod et al.⁴⁸ related such behavior to a “fragile-to-strong transition”. A main goal of the present work is to quantify the evolution of SHD during this crossover. Moreover, by means of quantitative comparison with literature data, we seek to ascertain differences and similarities of SHD among fragile and strong liquids, respectively. We study spatial correlations both between highly mobile particles and between highly immobile particles. Finally, we analyze the relation between properties of the local instantaneous liquid structure and the particle mobility, to investigate whether there is a structural origin of SHD in silica. Indications of a relationship between local structure and local dynamics have been demonstrated in the Dzugutov^{29,53} and BLJ liquids.²²

II. MODEL AND SIMULATION

Previous MD simulation studies^{43,44,45,46,47,48,49,50,51} have shown that the BKS potential⁴² is well suited to reproduce many structural and dynamical properties of amorphous silica. The BKS potential energy is given by

$$\phi_{\alpha\beta}(r) = \frac{q_\alpha q_\beta e^2}{r} + A_{\alpha\beta} \exp(-B_{\alpha\beta} r) - \frac{C_{\alpha\beta}}{r^6} \quad (1)$$

where r is the distance between two atoms of types α and β ($\alpha, \beta \in \{\text{Si}, \text{O}\}$) and e denotes the elementary charge. The partial charges q_α together with the potential parameters $A_{\alpha\beta}$, $B_{\alpha\beta}$ and $C_{\alpha\beta}$ can be found elsewhere.^{42,49}

Here, we follow simulations of Horbach and Kob^{44,45} and perform computations in the NVE ensemble where $N = 8016$ and $\rho = 2.37 \text{ g/cm}^3$ corresponding to a box length $L = 48.4 \text{ \AA}$. This system size is sufficiently large so as to avoid significant finite size effects at the studied T .^{50,51} The equations of motion are integrated using the velocity Verlet algorithm with a time step of 1.6 fs. In doing so, we truncate the non-Coulombic part of the potential at a cutoff radius of 5.5 \AA . The Coulombic part is calculated via Ewald summation⁵⁴ where we apply a parameter $\alpha = 0.265$ together with a cutoff in Fourier space $k_c = 2\pi/L\sqrt{51}$. As was discussed in previous work,^{44,45} the use of this value of k_c leads to a constant shift of the total potential energy and, hence, does not affect the forces. We consider values of T in a range between 3030 K and 5250 K, where the system is equilibrated for times longer than the structural relaxation time prior to data accumulation.

Horbach and Kob^{44,45} showed that BKS silica consists of a network of well defined silicate tetrahedra. Further, they analyzed the temperature dependences of the diffusion coefficient D and the time constant τ of the structural relaxation. At relatively high T , these quantities were found to vary according to a power-law

$$D, \tau^{-1} \propto (T - T_{MCT})^\gamma, \quad (2)$$

as predicted by MCT.¹³ For the critical temperature, Horbach and Kob^{44,45} reported $T_{MCT} = 3330$ K, in good agreement with $T_{MCT} = 3221$ K determined from experimental viscosity data of silica.⁵² The critical exponents extracted from $D(T)$ and $\tau^{-1}(T)$ were found to be $\gamma \approx 2.1$ and $\gamma \approx 2.4$, respectively.^{44,45} At T below a dynamical crossover in the vicinity of T_{MCT} , Arrhenius laws

$$D, \tau^{-1} \propto \exp[-E_a/(k_B T)] \quad (3)$$

were observed.^{44,45} Activation energies $E_a = 4.7$ eV and $E_a = 5.2$ eV for the oxygen and silicon atoms, respectively, were obtained from $D(T)$. The temperature dependence $\tau^{-1}(T)$, extracted from the incoherent intermediate scattering functions for the oxygen atoms, yielded activation energies between 5.0 eV and 5.5 eV, depending on the wave vector q . All these values are similar to $E_a = 4.7$ eV for oxygen and $E_a = 6.0$ eV for silicon observed in experimental studies near T_g .^{55,56}

Our analysis confirms these findings of Horbach and Kob.^{44,45} Specifically, our data are consistent with $T_{MCT} = 3330$ K and we obtain critical exponents $\gamma \approx 2.0$ and $\gamma \approx 2.2$ from $D(T)$ and $\tau^{-1}(T)$, respectively. Furthermore, we observe comparable activation energies, see section III A.

III. RESULTS

A. Properties of the bulk

To mark the various time regimes of the structural relaxation in BKS silica, we first discuss the incoherent intermediate scattering function

$$F_s(q, \Delta t) = \langle \cos\{\vec{q}[\vec{r}_i(t_0 + \Delta t) - \vec{r}_i(t_0)]\} \rangle. \quad (4)$$

Here, $\vec{r}_i(t_0)$ is the position of particle i at time t_0 and the brackets $\langle \dots \rangle$ denote the ensemble average. Figure 1 shows $F_s(q, \Delta t)$ for the oxygen and silicon atoms, respectively, where we use an absolute value of the wave vector, $q = 1.7 \text{ \AA}^{-1}$. This value of q corresponds to the first sharp diffraction peak of the static structure factor⁴⁴ and, hence, dynamics on the length scale of the distance of the silicate tetrahedra is probed. We see in Fig. 1 that the scattering functions for both atomic species are comparable. Typical of viscous liquids, $F_s(q, \Delta t)$ shows a two-step decay. While the short-time decay can be ascribed to ballistic motion, the non-exponential long-time decay results from the structural relaxation. As a consequence

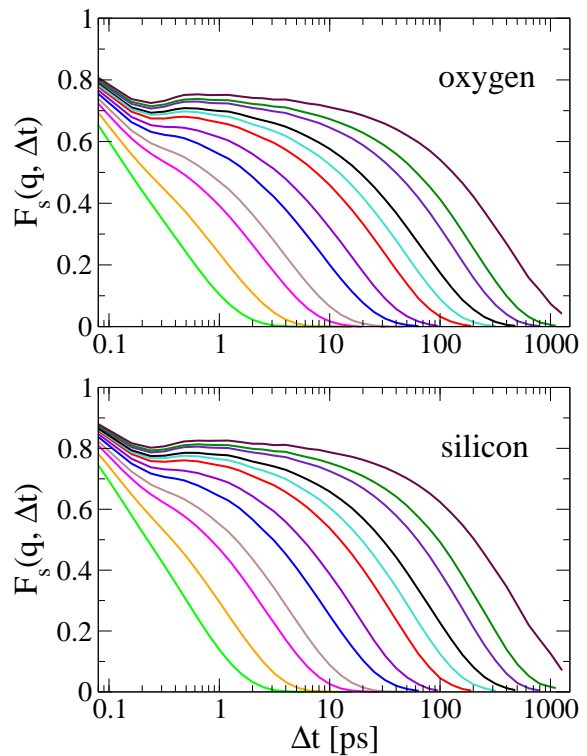


FIG. 1: Incoherent intermediate scattering functions, $F_s(q = 1.7 \text{ \AA}^{-1}; \Delta t)$, for the oxygen and silicon atoms, respectively. The temperatures are, from left to right: 5250 K, 4730 K, 4330 K, 4120 K, 3870 K, 3710 K, 3520 K, 3420 K, 3330 K, 3230 K, 3140 K and 3030 K.

of the cage effect,¹³ which describes that the particles are temporarily trapped in a cage formed by their neighbors, a plateau regime develops between the ballistic and diffusive regimes upon cooling. At the crossover from the ballistic to the plateau regime, the curves show oscillations that are damped out for longer times. Horbach *et al.*^{50,51} found a similar behavior and ascribed it to the Boson peak. However, the origin of this feature is still a matter of debate.^{45,57}

For an analysis of the structural relaxation, we fit the long-time decay of $F_s(q, \Delta t)$ to a Kohlrausch-Williams-Watts (KWW) function, $A \exp[-(t/\tau)^\beta]$. In Fig. 2, it is evident that the temperature dependence of the mean time constant, given by $\langle \tau \rangle = (\tau/\beta)\Gamma(1/\beta)$, is similar for both atomic species. At $T \lesssim 3300$ K, the data are well described by an Arrhenius law where we find activation energies $E_a = 5.0$ eV and $E_a = 5.1$ eV for the oxygen and silicon atoms, respectively. In contrast, there are deviations from an Arrhenius law at higher T , reflecting the crossover observed for the temperature dependence of the transport coefficients.^{40,44,48} In particular, $\langle \tau(T) \rangle$ can be fitted by Eq. 2 with $T_{MCT} = 3330$ K at $T > 3900$ K. The non-exponentiality of the structural relaxation can be quantified by the stretching parameter β of the KWW function. We observe $\beta > 0.8$ for all studied T and for both atomic species, and, hence, the devia-

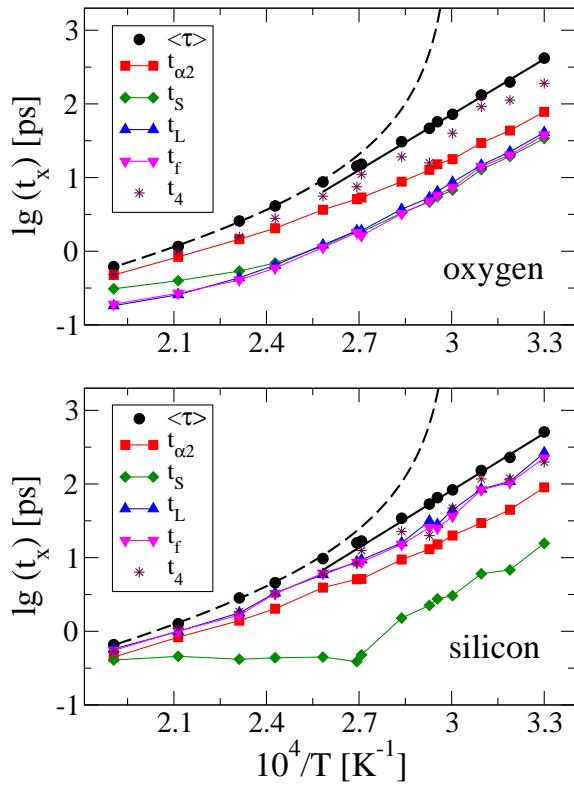


FIG. 2: Various time constants characterizing the dynamics of the oxygen and silicon atoms in BKS silica, see text for details. The data $\langle \tau(T) \rangle$ are fit by a power-law at $T > 3900$ K (dashed lines, Eq. 2 with $T_{MCT} = 3330$ K, $\gamma = 2.2$ for oxygen and silicon) and by an Arrhenius law at $T < 3300$ K (solid lines, Eq. 3, $E_a = 5.0$ eV for oxygen, $E_a = 5.1$ eV for silicon).

tions from an exponential behavior are small. A closer inspection reveals that starting from $\beta \approx 1$ at high T the stretching parameter first decreases, and then becomes constant within statistical error at $T \lesssim 3800$ K (oxygen: $\beta = 0.83 \pm 0.02$, silicon: $\beta = 0.85 \pm 0.02$).

Next, we study the self part of the van Hove correlation function

$$G_s(\vec{r}, \Delta t) = \langle \delta [\vec{r}_i(t_0 + \Delta t) - \vec{r}_i(t_0) - \vec{r}] \rangle. \quad (5)$$

The quantity $4\pi r^2 G_s(r, \Delta t)$ measures the probability that a particle moves a distance r in a time interval Δt . Figure 3 depicts this probability for the oxygen atoms at $T = 3230$ K. It is instructive to compare $G_s(r, \Delta t)$ with the Gaussian approximation^{20,22,34}

$$G_0(r, \Delta t) = \left(\frac{3}{2\pi \langle r_i^2(\Delta t) \rangle} \right)^{\frac{3}{2}} \exp \left(-\frac{3}{2 \langle r_i^2(\Delta t) \rangle} \right) \quad (6)$$

where $r_i^2(\Delta t) = |\vec{r}_i(t_0 + \Delta t) - \vec{r}_i(t_0)|^2$. While $G_s(r, \Delta t) = G_0(r, \Delta t)$ for short and long times in the structural relaxation process, significant deviations are obvious at intermediate times. They are demonstrated for $\Delta t = 31.8$ ps in Fig. 3. For this time interval, $4\pi r^2 G_s(r, \Delta t)$ shows a pronounced tail, indicating that some particles move

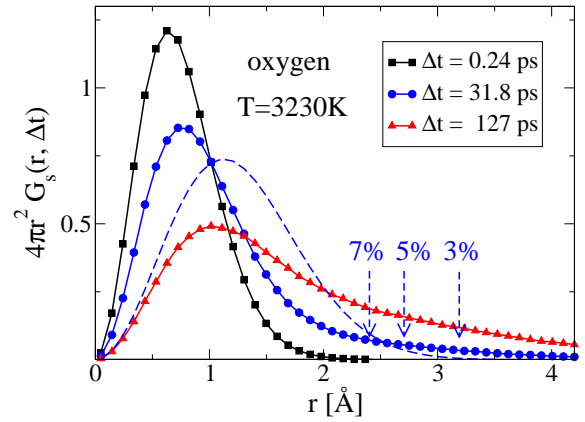


FIG. 3: Self part of the van Hove correlation function, $G_s(r, \Delta t)$, for the oxygen atoms in BKS silica at $T = 3230$ K. The time $\Delta t = 31.8$ ps compares to the transition between the plateau and diffusive regimes. Dashed line: Gaussian approximation $G_0(r, \Delta t)$ for $\Delta t = 31.8$ ps, cf. Eq. 6. The arrows indicate the distances r_c for which the integral $\phi = \int_{r_c}^{\infty} 4\pi r^2 G_s(r, \Delta t = 31.8 \text{ ps}) dr$ equals 3%, 5% and 7%, respectively. The data to the right of the arrows result from highly mobile particles studied in section III B. For comparison, the oxygen-oxygen interparticle distance r_{OO} equals 2.6 \AA , see Fig. 11

much farther than expected from a Gaussian approximation. Such behavior is well known from previous studies of fragile viscous liquids.^{20,22,30,34,35,36,37} In the present system, we observe this behavior also at T below the fragile-to-strong crossover, consistent with previous findings.⁴⁴ This result gives a first indication of a similarity in SHD between fragile and strong liquids.

The deviations from Gaussian behavior can be quantified by the non-Gaussian parameter^{22,35}

$$\alpha_2(\Delta t) = \frac{3}{5} \frac{\langle r_i^4(\Delta t) \rangle}{\langle r_i^2(\Delta t) \rangle^2} - 1. \quad (7)$$

In Fig. 4, we see that $\alpha_2(\Delta t)$ exhibits a maximum at intermediate times. For both atomic species, the position of the maximum, $t_{\alpha 2}$, shifts to longer times and the maximum value, $\alpha_2^m \equiv \alpha_2(t_{\alpha 2})$, increases with decreasing T . The insets of Fig. 4 demonstrate that the increase of α_2^m can be described by an exponential growth with $1/T$. For the silicon atoms, the temperature dependence may be weaker at $T \lesssim T_{MCT}$, but statistics are too poor to draw unambiguous conclusions. In any case, the data show that the crossover observed for the transport coefficients is not of great importance for the temperature dependence of α_2^m . At any given T , the non-Gaussian parameter is larger for oxygen than for silicon, implying that dynamic heterogeneity is more pronounced for oxygen. The temperature dependence of $t_{\alpha 2}$ is displayed in Fig. 2. Upon cooling, $t_{\alpha 2}$ decouples from $\langle \tau \rangle$ so that the time constants differ by about one order of magnitude at $T = 3030$ K. Comparison with Fig. 1 shows

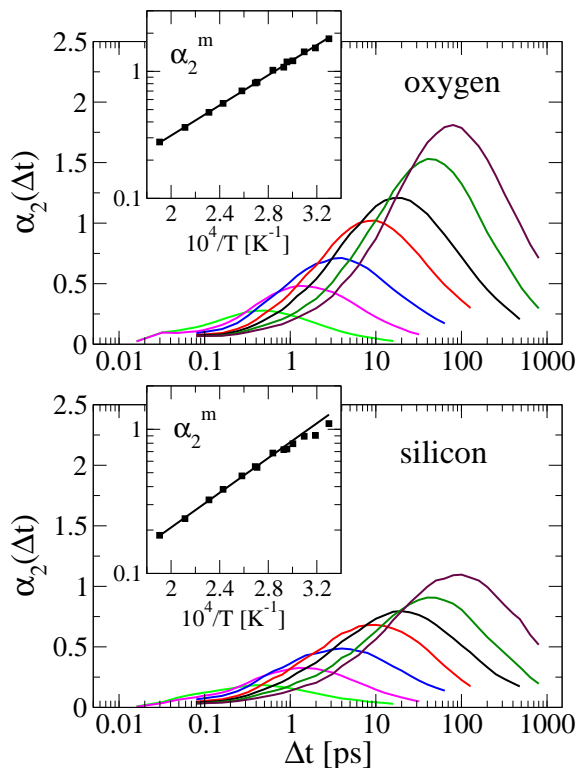


FIG. 4: Non-Gaussian parameter $\alpha_2(\Delta t)$ for the oxygen and silicon atoms at various temperatures (5250 K, 4330 K, 3870 K, 3520 K, 3330 K, 3140 K, 3030 K). The insets show the temperature dependence of the maximum values, α_2^m . The solid lines are interpolations of the data at $T > 3600$ K with an Arrhenius law. The limited fitting range was chosen to determine whether α_2^m shows a significantly different temperature dependence at low temperatures.

that the deviations from Gaussian behavior are largest in the late- β / early- α relaxation regime, consistent with previous results for various models of supercooled liquids.^{20,22,30,34,35,36,37}

B. Properties of highly mobile particles

In this section, we investigate the properties of highly mobile particles on intermediate time scales. Since we are interested in a detailed comparison with results for non-networked glass forming liquids, our analysis focuses on quantities studied in previous work.^{22,30,34,37,38} There, fractions of mobile particles $\phi = 5 - 7\%$ were considered. These fractions were obtained as the fractions of particles in the tail of $G_s(r, t_{\alpha 2})$. Note that these highly mobile particles show displacements of at least one interparticle distance, while the rest of the particles are trapped in their local cages, see Fig. 3. Here, we compare results for $\phi = 3\%$, $\phi = 5\%$ and $\phi = 7\%$, where the most mobile particles in a time interval Δt are identified based on the scalar particle displacements within this time window. We analyze the behavior of the oxygen and silicon atoms

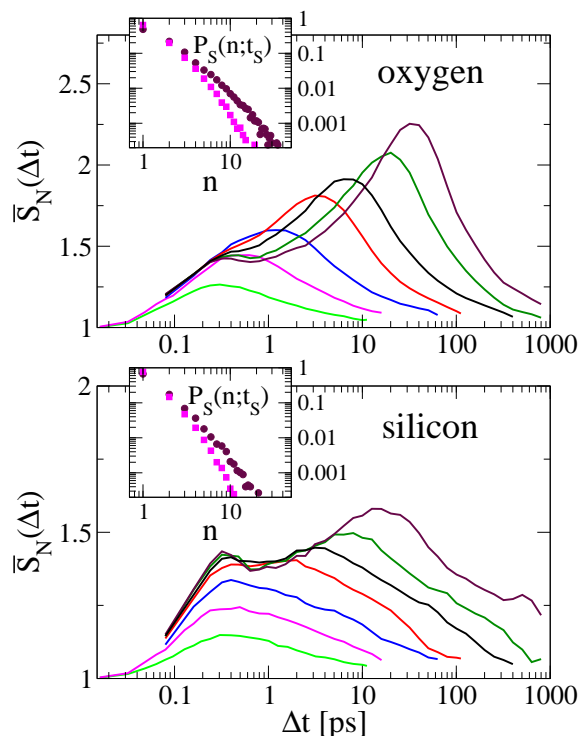


FIG. 5: Normalized number-averaged mean cluster size, $\bar{S}_N(\Delta t)$, for the oxygen and silicon atoms at various temperatures (5250 K, 4330 K, 3870 K, 3520 K, 3330 K, 3140 K, 3030 K) and a fraction $\phi = 5\%$. The insets show the probability distribution of the cluster size, $P_S(n; \Delta t)$, for $T = 3030$ K and $T = 4330$ K, and times when the mean cluster size is a maximum ($\Delta t = t_S$).

separately, since the atomic species exhibit somewhat different properties, as shown below.

1. Clusters

To ascertain the spatially heterogeneous nature of dynamics in BKS silica we first show that highly mobile particles form clusters larger than expected from random statistics. Following previous studies,^{22,30,34,37,38,40} we define a cluster as a group of highly mobile particles that reside in the first neighbor shells of each other. For both atomic species, we define the neighbor shell based on the first minimum of the respective pair correlation function. A statistical analysis of the clusters is possible when we determine the probability distribution $P_S(n; \Delta t)$ of finding a cluster of size n for a time interval Δt . From this distribution, the number-averaged and weight-averaged mean cluster size can be calculated according to

$$S_N(\Delta t) = \sum_n n P_S(n; \Delta t) \quad (8)$$

and

$$S_W(\Delta t) = \frac{\sum_n n^2 P_S(n; \Delta t)}{\sum_n n P_S(n; \Delta t)}, \quad (9)$$

respectively, where $\sum_n P_S(n) = 1$.

In the following analysis of the clusters and, later, of the strings, we focus on the number-averaged data for the fraction $\phi = 5\%$. Here, the number average is considered due to the smaller statistical error of this quantity. However, we carefully checked that our conclusions depend neither on the average nor the fraction considered. For several examples, this is demonstrated by including results for $\phi = 3\%$ and $\phi = 7\%$. Some findings for the weight-averaged data were shown in previous work.⁴⁰ They are discussed in section IV, when we compare SHD in various models of viscous liquids on a quantitative level. Finally, we determined that an analysis of clusters consisting of both mobile oxygen and silicon atoms does not yield new insights.

In Fig. 5, we display the temperature dependence of the normalized mean cluster size $\bar{S}_N(\Delta t) = S_N(\Delta t)/S_N^*$, where $S_N^* = 1.21$ is the mean cluster size resulting when 5% of the particles are randomly chosen to construct clusters. Thus, $\bar{S}_N(\Delta t)$ measures exclusively effects due to SHD. Inspecting the oxygen data, we see that $\bar{S}_N(\Delta t)$ exhibits a peak, indicating the existence of clusters that are transient in nature. This peak grows and shifts to longer times upon cooling. In addition, there is a shoulder near $\Delta t \approx 0.3$ ps. These findings confirm our previous results for the corresponding weight-averaged data, $\bar{S}_W(\Delta t)$.⁴⁰ For silicon, the shoulder becomes a separate maximum and $\bar{S}_N(\Delta t)$ shows two peaks at low T . Since the position and height of the primary maximum depend more strongly on temperature than those of the secondary maximum, both peaks merge at high T . Comparing the data for both atomic species, we observe that the clusters are larger for oxygen, consistent with a larger value of α_2^m for this species.

A shoulder in $\bar{S}_N(\Delta t)$ at the crossover from the ballistic to the plateau regime was also observed for water,³⁷ whereas such an increase is absent in simple liquids^{22,30,38} and a polymer melt.³⁴ In the case of water,³⁷ this phenomenon was ascribed to “strong correlations in the vibrational motion of first-neighbor molecules, owing to the presence of hydrogen bonds”. Similarly, we suggest that the network structure of silica enables a collective vibrational mode, which becomes more relevant when T is decreased. This conclusion is corroborated by the oscillatory behavior of $F_s(q, \Delta t)$ in the corresponding time regime, see Fig. 1. Provided these findings for silica can be attributed to the Boson peak, as proposed by Horbach *et al.*,^{50,51} our findings imply that this phenomenon results from a local, collective vibration.

SHD related to the structural relaxation manifests itself in the primary maximum of $\bar{S}_N(\Delta t)$. For a quantitative analysis, we extract the peak times and peak heights. In Fig. 2, we see that the mean cluster size is maximum at times $t_S \ll \langle \tau \rangle$, where the ratio $\langle \tau \rangle / t_S$ is nearly independent of T . For the silicon atoms, such analysis is not possible at sufficiently high T , because the primary maximum is submerged by the secondary maximum so that the temperature-independent position of the latter

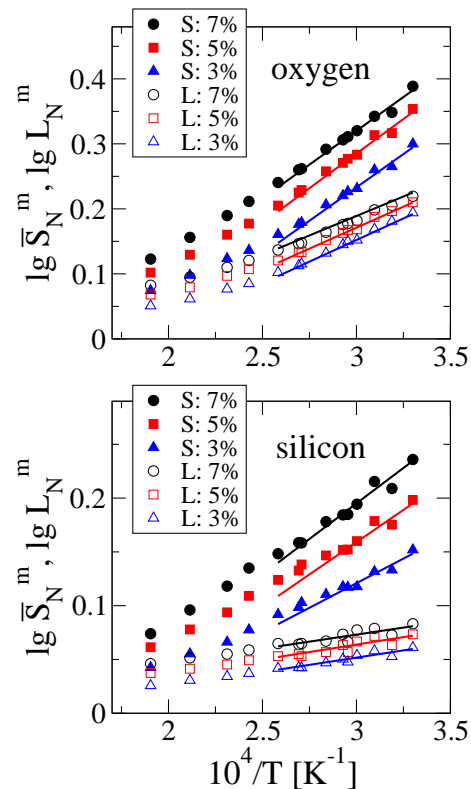


FIG. 6: Maximum of the normalized mean cluster size, \bar{S}_N^m , together with the maximum of the mean string length, L_N^m , for the oxygen and silicon atoms as a function of the reciprocal temperature. The various fractions of mobile particles, ϕ , used in the analysis are indicated. The solid lines are guides to the eye.

results in a constant value for t_S . Despite slight deviations, the temperature dependence of t_S for different values of ϕ is comparable. Specifically, t_S increases with increasing percentage, but the data for $\phi = 3\%$ and $\phi = 7\%$ differ by less than a factor of 2 at all studied T . In Fig. 6, we show the temperature dependence of the peak height $\bar{S}_N^m \equiv \bar{S}_N(t_S)$ for all considered fractions ϕ . Inspecting the data for the lower T , we observe that \bar{S}_N^m grows nearly exponentially with increasing $1/T$. Thus, even in a temperature range where the relaxation time $\langle \tau \rangle$ varies according to an Arrhenius law, the cluster size strongly increases. A more detailed analysis together with a discussion of the results will be presented in section III C.

Finally, we investigate the probability distribution of the cluster size, $P_S(n; \Delta t)$. For simple liquids^{22,30,38} and a polymer melt,³⁴ this distribution exhibits a power-law behavior when $\Delta t = t_S$ and $T \approx T_{MCT}$. In the insets of Fig. 5, we show $P_S(n; t_S)$ for the oxygen and silicon atoms at representative values of T . At $T = 3030$ K, clusters containing as many as 40 oxygen atoms and 20 silicon atoms are observed. However, a power-law is not found in the studied temperature range, indicating that this feature of SHD in simple liquids cannot be generalized to the case of the network-former BKS silica. The

data can be satisfactorily fit by a power-law multiplied by an exponential cutoff. Such behavior is expected when a percolation transition is approached and, hence, we cannot exclude that such a transition occurs at much lower T .

2. Strings

It has been demonstrated^{21,22,30,35} that dynamics in several fragile liquids are facilitated by string-like motion, i.e., groups of particles follow each other along one-dimensional paths. However, our previous work⁴⁰ suggests that this type of motion is less important for silica. To study the relevance of string-like motion in more detail, we follow Donati *et al.*²¹ and construct strings by connecting any two particles i and j of the same atomic species if

$$\min[|\vec{r}_i(t_0) - \vec{r}_j(t_0 + \Delta t)|, |\vec{r}_i(t_0 + \Delta t) - \vec{r}_j(t_0)|] < \delta.$$

Similar to the values used in previous work^{21,22,30,35}, we set δ to $\sim 55\%$ of the respective interatomic distance, resulting in $\delta = 1.4 \text{ \AA}$ and $\delta = 1.7 \text{ \AA}$ for oxygen and silicon, respectively. Then, the above condition implies that one particle has moved and another particle has occupied its position. We checked that our conclusions are not affected when δ is varied in a meaningful range.

For an analysis of string-like motion, we determine the probability distribution $P_L(l; \Delta t)$ of finding a string of length l in a time interval Δt and calculate the number-averaged mean string length $L_N(\Delta t)$ in analogy with Eq. 8. Note that we include “strings” containing only one atom. In Fig. 7, we display the temperature dependence of $L_N(\Delta t)$. Though the strings for both atomic species grow and shrink in time, string-like motion is very different for the oxygen and silicon atoms. We see that, at any given T , $L_N(\Delta t)$ is maximum at a much later time for silicon than for oxygen. Further, the mean string length is significantly smaller for the former than for the latter atomic species. In particular, for the silicon atoms, the small values $L_N(\Delta t) \approx 1$ imply very limited string-like motion.

The different behavior of the oxygen and silicon atoms can be quantified by the peak times t_L and peak heights $L_N^m \equiv L_N(t_L)$. The former are included in Fig. 2. For oxygen, we find that the mean string length and the mean cluster size are maximum at similar times $t_S \approx t_L \ll \langle \tau \rangle$, as was observed for simple liquids^{22,30} and a polymer melt.³⁵ In contrast, these mean sizes peak at very different times for silicon where the few short strings are largest in the α -relaxation regime, i.e., $t_S \ll t_L \approx \langle \tau \rangle$. This finding clearly shows that the string-like motion known for fragile liquids is suppressed for the silicon atoms. In Fig. 6, we show the temperature dependence of the peak heights L_N^m for all studied fractions ϕ . As was observed for the clusters, the mean string size for the oxygen atoms increases nearly exponentially with $1/T$ at the lower T . For the silicon atoms, the strings grow more

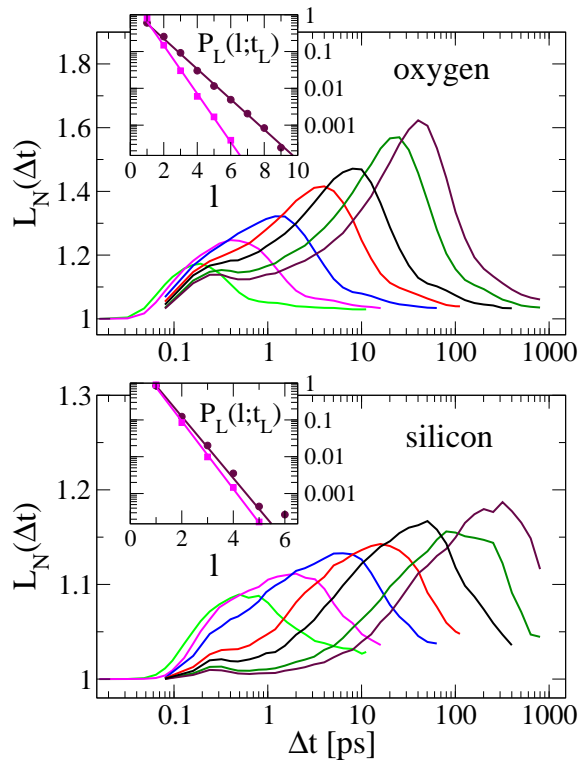


FIG. 7: Number-averaged mean string length, $L_N(\Delta t)$, for the oxygen and silicon atoms at various temperatures (5250 K, 4330 K, 3870 K, 3520 K, 3330 K, 3140 K, 3030 K), where $\phi = 5\%$. The insets show the probability distribution of the string length, $P_L(l; \Delta t)$, for $T = 3030 \text{ K}$ and $T = 4330 \text{ K}$, and times when the mean string size is a maximum ($\Delta t = t_L$).

slowly, but large scattering of the data, in particular at low T , hampers a quantification of the temperature dependence.

Examples of the probability distribution of the string length, $P_L(l, \Delta t)$, are shown in the insets of Fig. 7. For all considered T and both atomic species, $P_L(l, \Delta t)$ decays exponentially when $\Delta t = t_L$, as was observed in previous studies of string-like motion.^{21,22,30,35} This finding suggests that an exponential distribution $P_L(n, t_L)$ is a feature inherent to strings constructed in the way described above. In view of the exponential distribution, an analogy to the equilibrium polymerization of linear polymers was proposed in previous work.^{21,35}

Finally, we analyze the relevance of string-like motion for the relaxation of the most mobile particles in silica. Following previous work,³⁰ we quantify the importance by the fraction of mobile particles, $f(\Delta t)$, that are involved in non-trivial strings, i.e., strings with $l \geq 3$. In Fig. 8, we see that string-like motion is of very limited relevance for silicon, whereas it becomes increasingly important for oxygen upon cooling. Hence, this dynamical pattern may be an important channel of relaxation for oxygen near T_g . A more detailed analysis reveals that $f(\Delta t)$ is maximum at times $\Delta t = t_f \approx t_L$ for both the oxygen and the silicon atoms, see Fig. 2. Inspecting the

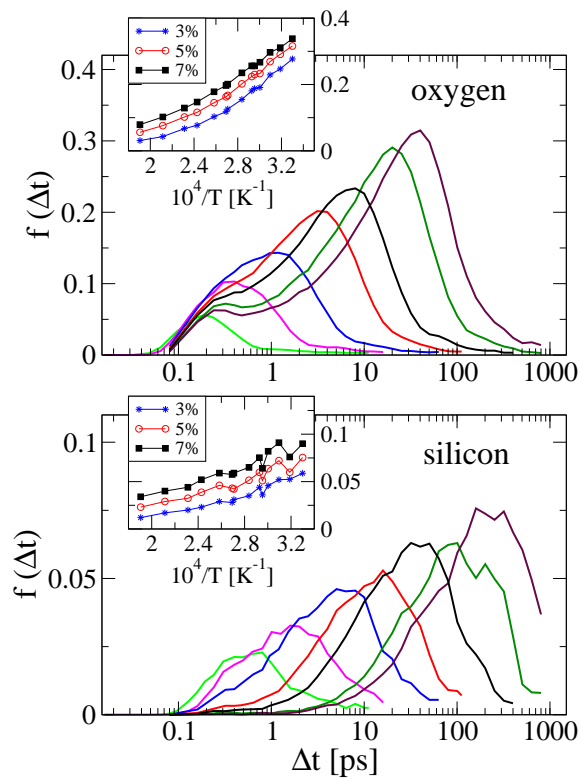


FIG. 8: Fraction $f(\Delta t)$ of highly mobile oxygen and silicon atoms, respectively, that are involved in non-trivial string-like motion ($l \geq 3$). We display results for 5250 K, 4330 K, 3870 K, 3520 K, 3330 K, 3140 K and 3030 K. The insets show the maximum value, f^m , as a function of the reciprocal temperature. The values of ϕ used in the analysis are indicated.

maximum amplitude f^m in the insets of Fig. 8, it is evident that our conclusions do not depend on the value of ϕ .

C. Relation to the Adam-Gibbs theory

The Adam-Gibbs (AG) relation⁷ $D \propto \exp[-A/(TS_c)]$, which links the diffusion coefficient with the configurational entropy S_c , was found to hold for a BLJ liquid,⁵⁸ water⁵⁹ and the present case of BKS silica.⁴⁸ The AG theory further proposes a relation between S_c and the characteristic mass of cooperatively rearranging regions (CRR). However, the CRR are not precisely defined in the theory and their nature is still elusive. In recent work on water, Giovambattista *et al.*³⁷ observed that

$$(S_N^m - 1) \propto 1/S_c, \quad (10)$$

suggesting that, first, the (non-normalized) mean cluster size is a measure of the mass of the CRR and, second, a cluster of size one does not correspond to a CRR. Furthermore, they confirmed along the considered isochore the expectation

$$D \propto \exp[-A^*(S_N^m - 1)/T] \quad (11)$$

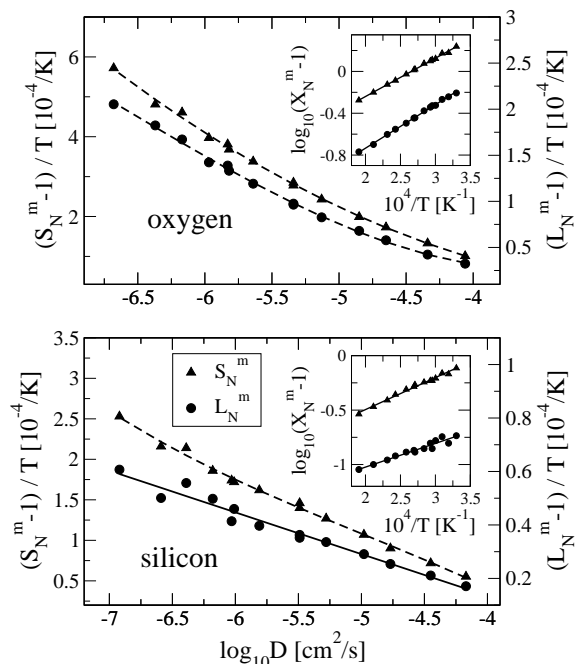


FIG. 9: $S_N^m - 1$ and $L_N^m - 1$ as a function of the logarithm of the diffusion coefficient D . The dashed lines are guides to the eye. The solid line is a linear interpolation, which will be expected if clusters or strings are related to the cooperatively rearranging regions of the Adam-Gibbs theory.^{37,60} In the insets, we depict the temperature dependence of $X_N - 1 \equiv S_N^m - 1$, $L_N^m - 1$ together with Arrhenius fits (solid lines).

resulting from the AG relation together with Eq. 10.

Here, we analyze whether Eq. 11 is valid for BKS silica. Since the AG relation holds for this model in the studied temperature range,⁴⁸ the validity (failure) of Eq. 11 implies the validity (failure) of Eq. 10 and, hence, we can determine whether a relation between the clusters of mobile particles and the CRR exists, as was reported for water.³⁷ To this end, we extract the diffusion coefficient from the long-time behavior of the mean square displacement⁴⁰ and plot $(S_N^m - 1)/T$ as a function of $\log D$ in Fig. 9. Evidently, a linear relation is observed for neither oxygen nor silicon, indicating a failure of Eq. 11 and, thus, also Eq. 10. Hence, for silica, the mean cluster size S_N^m is not a measure of the characteristic mass of the CRR. We also find that such relation is not valid for the weight-averaged data S_W^m or for clusters consisting of both oxygen and silicon atoms. On the other hand, it has been argued^{30,38,60} that the strings and not the clusters are the elementary units of cooperative motion and, hence, related to the CRR. Therefore, we include $(L_N^m - 1)/T$ as a function of $\log D$ in Fig. 9. While no linear relation is found for the oxygen atoms, such behavior cannot be ruled out for the silicon atoms. However, the variation of L_N^m is too small to draw any conclusion in the latter case, where string-like motion is peculiar and largely insignificant anyway.

In the insets of Fig. 9, we show the temperature depen-

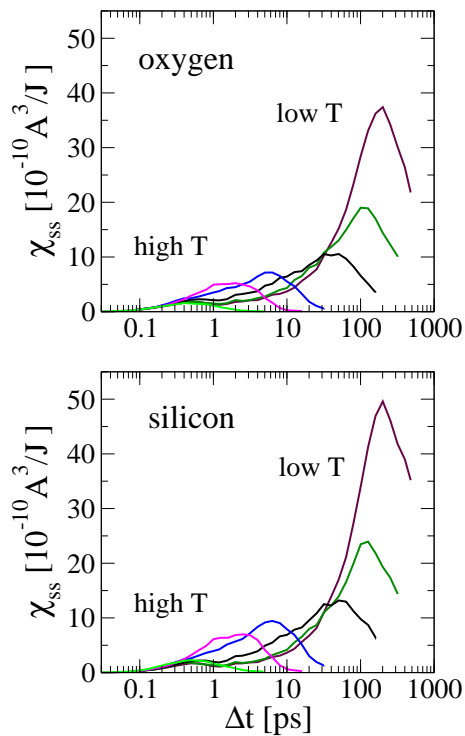


FIG. 10: Generalized susceptibility $\chi_{ss}(\Delta t)$ for the oxygen and silicon atoms. The temperatures are 5250 K, 4330 K, 3870 K, 3330 K, 3140 K and 3030 K.

dence of $S_N^m - 1$ and $L_N^m - 1$. For both atomic species, we observe that an exponential growth with $1/T$ fits the data well over the entire temperature range. This behavior is confirmed by our analysis for the fractions $\phi = 3\%$ and $\phi = 7\%$ (not shown), indicating that, in a strong glass former, SHD becomes increasingly important with decreasing T . In particular, we find no evidence for substantial effects due to the “fragile-to-strong crossover” observed for the transport coefficients. Provided the exponential growth continues upon further cooling, the mean cluster and mean string size are finite at all finite T . In contrast, a power-law temperature dependence of the mean cluster size was found for a BLJ liquid,^{22,38} suggesting a percolation transition of clusters of mobile particles in the vicinity of T_{MCT} .

D. Behavior of four-point spatiotemporal density fluctuations

Previous work^{24,25,26,27,39} showed that two-point, two-time fourth order density correlation functions are well suited to study SHD. The general theoretical framework is described in detail in the literature.^{26,28} In brief, it has been proven useful to define an “order parameter” $Q(\Delta t)$ that compares the configurations of a liquid with density

$\rho(\vec{r}, t) = \sum_{i=1}^N \delta(\vec{r} - \vec{r}_i(t))$ at two different times $\Delta t \equiv t_2 - t_1$

$$\begin{aligned} Q(\Delta t) &= \int d^3 r_1 d^3 r_2 \rho(\vec{r}_1, 0) \rho(\vec{r}_2, \Delta t) \cos[\vec{q}(\vec{r}_1 - \vec{r}_2)] \\ &= \sum_{i=1}^N \sum_{j=1}^N \cos[\vec{q}(\vec{r}_i(0) - \vec{r}_j(\Delta t))]. \end{aligned} \quad (12)$$

$Q(\Delta t)$ counts the number of “overlapping” particles in two configurations separated by a time interval Δt . Here, we do not apply a strict cutoff to define overlapping particles, as was done in previous studies,^{24,25,26} but we follow Berthier²⁷ and use the intermediate scattering function, $\cos[\vec{q}(\vec{r}_1 - \vec{r}_2)]$, where we again choose $q = 1.7 \text{ \AA}^{-1}$. The fluctuations of this quantity are described by a generalized susceptibility

$$\chi_4(\Delta t) = \frac{\beta V}{N^2} [\langle Q^2(\Delta t) \rangle - \langle Q(\Delta t) \rangle^2], \quad (13)$$

which corresponds to the volume integral of a four-point density correlation function

$$\begin{aligned} \chi_4(\Delta t) &= \frac{\beta V}{N^2} \int d^3 r_1 d^3 r_2 d^3 r_3 d^3 r_4 \cos[\vec{q}(\vec{r}_1 - \vec{r}_2)] \\ &\quad \times \cos[\vec{q}(\vec{r}_3 - \vec{r}_4)] G_4(\vec{r}_1, \vec{r}_2, \vec{r}_3, \vec{r}_4, \Delta t) \end{aligned} \quad (14)$$

where $\beta = k_B T$ and

$$\begin{aligned} G_4(\vec{r}_1, \vec{r}_2, \vec{r}_3, \vec{r}_4, t) &= \langle \rho(\vec{r}_1, 0) \rho(\vec{r}_2, t) \rho(\vec{r}_3, 0) \rho(\vec{r}_4, t) \rangle \\ &\quad - \langle \rho(\vec{r}_1, 0) \rho(\vec{r}_2, t) \rangle \langle \rho(\vec{r}_3, 0) \rho(\vec{r}_4, t) \rangle. \end{aligned}$$

The overlapping particles are comprised of localized particles that have hardly moved and particles that have been replaced by a neighboring particle. Accordingly, χ_4 can be decomposed into self- (χ_{SS}), distinct- (χ_{DD}) and interference (χ_{SD}) parts, where the main contribution was found to result from the self part.^{24,26} In this section, we are interested in spatial correlations of highly immobile particles. Therefore, we focus on the self part, which is given by

$$\chi_{SS}(\Delta t) = \frac{\beta V}{N^2} [\langle Q_S^2(\Delta t) \rangle - \langle Q_S(\Delta t) \rangle^2], \quad (15)$$

where

$$Q_S(\Delta t) = \sum_{i=1}^N \cos[\vec{q}(\vec{r}_i(0) - \vec{r}_i(\Delta t))]. \quad (16)$$

In Fig. 10, we show $\chi_{SS}(\Delta t)$ for the oxygen and silicon atoms at several values of T . While the susceptibility is small at high T , it shows a pronounced maximum at low T . This strong increase of the peak height, χ_4^m , indicates a growing range of spatial correlations between immobile particles with decreasing T .^{24,25,26,27} Unfortunately, a detailed analysis of the temperature dependence of χ_4^m is hampered by a large scattering of the values (not shown). To characterize the times when the fluctuations in the number of localized particles are biggest,

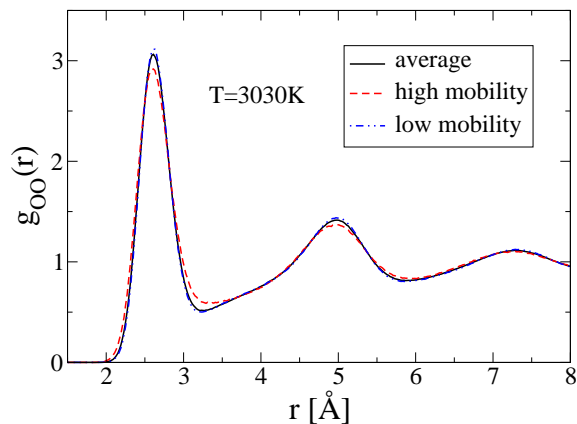


FIG. 11: Pair correlation functions $g_{OO}(r)$ at $T = 3030$ K. We compare results obtained for all oxygen atoms with those for the most mobile and the most immobile oxygen atoms in a time interval $\Delta t = 10 \text{ ps} \approx t_S$, respectively.

we extract the peak times t_4 . From the results in Fig. 2, it is evident that, for both atomic species, the spatial correlations between highly immobile particles are maximum in the α -relaxation regime. In particular, $\langle \tau \rangle$ and t_4 show a very similar temperature dependence, where the ratio $\langle \tau \rangle / t_4$ amounts to a factor of about two. On the other hand, t_4 is about one order of magnitude longer than t_S and, hence, SHD analyzed from the perspectives of highly immobile and highly mobile particles, respectively, is most pronounced at different times. All these findings are consistent with previous results for BLJ liquids.^{24,25,26,27,28}

E. Relation between structure and dynamics

Amorphous silica consists of a network of well-defined silicate tetrahedra. Hence, one may speculate that high particle mobility is found where the local structure is distorted. To study the relation between structure and dynamics, we identify the most mobile and the most immobile particles during a time interval Δt and characterize their respective environments at the beginning of this period by means of the pair correlation functions (PCF), $g_{\alpha\beta}(r)$, and the distributions of coordination numbers, $z_{\alpha\beta}(n)$ ($\alpha, \beta \in \{\text{O}, \text{Si}\}$). In Fig. 11, we compare $g_{OO}(r)$ for the mobile and immobile oxygen atoms, where $\Delta t \approx t_S$ and $T = 3030$ K. While the data for the immobile particles are comparable to those for the ensemble average, the first and second neighbor peak are slightly broadened for the mobile oxygen atoms. This behavior is similar for all $g_{\alpha\beta}(r)$. Thus, mobile particles during a time interval Δt_S exhibit a somewhat less ordered local environment at the beginning of this time window, at least as measured by $g_{\alpha\beta}(r)$, but the effects are weak. A variation of Δt in a meaningful range does not change these conclusions.

Some of the results from our analysis of the distributions $z_{\alpha\beta}(n)$ are compiled in Table I, where the coordi-

	average	mobile
\bar{z}_{OO}	7.2	7.5
\bar{z}_{SiSi}	4.2	4.4
$z_{OSi}(n=2)$	0.99	0.94
$z_{SiO}(n=4)$	0.98	0.94

TABLE I: Coordination numbers characterizing the local structure in BKS silica at $T = 3030$ K.

nation number n is defined as the number of β atoms for which the distance from a given α atom is smaller than that corresponding to the first minimum of $g_{\alpha\beta}(r)$. It is evident that mobile oxygen and silicon atoms exhibit somewhat higher mean coordination numbers \bar{z}_{OO} and \bar{z}_{SiSi} , respectively, suggesting that their positions are less favorable in terms of the potential energy. Further, the percentage of mobile oxygen atoms in the “ideal” coordination with two silicon neighbors is smaller than for an average oxygen atom. Likewise, compared to an average particle, mobile silicon atoms are more often three- or fivefold coordinated to oxygen. However, the vast majority of the mobile particles are still in their preferred local structure at the beginning of the particular time interval and, hence, defects of the local structure are not a necessary precondition of high particle mobility. On the other hand, the observed correlations imply that a somewhat less ordered local environment facilitates particle dynamics. Thus, the relation between structure and dynamics in BKS silica is non-trivial, as was also observed for BLJ mixtures²² and the Dzugutov liquid.²⁹

IV. DISCUSSION

One goal of the present work is to compare dynamic heterogeneity in various model liquids. For this purpose, we show our results together with the corresponding literature data in Table II. To enable a quantitative comparison, we consider results for $T \approx T_{MCT}$ in each case. Inspecting the data, it becomes clear that there is a correlation between the properties of dynamic heterogeneity at intermediate times and the features of the α relaxation, e.g., the stretching parameter β characterizing the nonexponentiality of the decay of the incoherent intermediate scattering function. Specifically, the Dzugutov liquid shows the most pronounced dynamic heterogeneity at intermediate times and the smallest value of β , whereas systems like silica, with less heterogeneous dynamics at intermediate times, exhibit a larger β . In what follows, we discuss the findings for various model liquids in more detail.

First, we see from Table II that the non-Gaussian parameter α_2 attains the largest values for the non-network forming liquids. Though α_2 was found to characterize aspects of the heterogeneity of dynamics,³⁶ it does not provide direct information about the spatial arrangement of mobile and immobile particles. The spatially het-

	BLJ ₁	BLJ ₂	PM	DZ	H ₂ O	O	Si
β	0.75	0.55	0.70	0.50	0.75	0.83	0.85
α_2^m	1.6	2.0	1.3	2.5	1.3	1.3	0.8
S_W^m	15 (5)		16 (6.5)	22 (5)		7.9 (7)	3.9 (7)
\bar{S}_W^m			6.0 (6.5)	11(5)	4.2 (7)	4.9 (7)	2.8 (7)
L_N^m	2.2 (5)		1.9 (6.5)	2.4 (5)		1.5 (5)	1.1 (5)
f^m				0.70 (5)		0.24 (5)	0.07 (5)
χ_4^m	4.7	18					

TABLE II: Quantities characterizing dynamic heterogeneity in various model liquids at $T \approx T_{MCT}$. We compare data for a 80:20 binary Lennard-Jones mixture (BLJ₁, $T = 1.04 T_{MCT}$),^{21,22} a 50:50 binary Lennard-Jones mixture (BLJ₂, $T = T_{MCT}$),^{26,61} a polymer melt (PM, $T = 1.02 T_{MCT}$),^{34,35,62} the Dzugutov liquid (DZ, $T = 1.05 T_{MCT}$)^{30,60} and water (H₂O, $T = 1.04 T_{MCT}$)^{37,63} with the present results for the oxygen (O) and silicon (Si) atoms in BKS silica at $T = T_{MCT}$. The values in brackets denote the fractions of mobile particles, ϕ , used in the respective analysis (in percent).

erogeneous nature of dynamics in the vicinity of T_{MCT} can be studied by identifying clusters of mobile particles.^{22,30,34,37} On a qualitative level, the clusters in various model liquids, including BKS silica, show an analogous behavior. For example, the clusters strongly grow upon cooling, where, at each T , the mean cluster size is maximum at times t_S in the late- β / early- α relaxation regime. On a quantitative level, several findings for simple liquids^{22,30} and a polymer melt,^{34,35} e.g., a power-law distribution of the cluster size, cannot be generalized to the case of silica. Moreover, there is a spectrum of maximum mean cluster sizes, the higher and lower end of which are attained by the Dzugutov liquid and the network formers silica and water, respectively, see Tab. II. However, one has to consider that, with the same definition, see section III B, the sizes of the clusters depend on the properties of the local structure. Specifically, compared to simple liquids, the particles in network-forming liquids exhibit smaller coordination numbers and, hence, the probability that a mobile particle has a mobile neighbor is smaller. This means that, within the same definition, the clusters are less likely to grow. At least to some extent, these effects are canceled out when the mean cluster size is normalized by the value expected from random statistics. However, at the present time, it is not clear whether \bar{S}_N and \bar{S}_W allow one to study SHD completely independent of the local structure. In any case, a comparison of the results among the simple liquids, where the coordination numbers are similar, suggests a relation between the mean cluster size and the stretching parameter β .

A main difference between various model liquids is the relevance of string-like motion at $T \approx T_{MCT}$. From the mean string length L_N^m and the fraction f^m of mobile particles moving in non-trivial strings, it is evident that this type of motion is an important channel of relaxation in the Dzugutov liquid, but not in BKS silica, see Tab. II. Moreover, the two atomic species in silica behave differently. On the one hand, some string-like motion is observed for the oxygen atoms. In agreement with previous results,^{22,30,35} the mean string length is maximum at intermediate times $t_L \approx t_S$, where the peak height L_N^m

increases with decreasing T . Hence, despite a limited relevance at $T \approx T_{MCT}$, string-like motion may become important for the structural relaxation of the oxygen atoms near T_g , cf. Fig. 7. On the other hand, the silicon atoms do *not* show string-like motion at intermediate times. Instead, there are very few short strings at much later times $t_S \ll t_L \approx \langle \tau \rangle$, implying that their nature is different from that observed for other model liquids.^{22,30,35} Therefore, we conclude that the “usual” string-like motion is absent for the silicon atoms. When we also consider that the oxygen and silicon atoms typically exhibit two and four covalent bonds, respectively, our findings imply that string-like motion is suppressed by the presence of covalent bonds.

Giovambattista *et al.*³⁷ found for water that the diffusion coefficient D is related to the mean cluster size via the AG relation where the cluster size is a measure of the mass of the CRR. In particular, they showed that a linear relation exists between $\log D$ and $S_N^m - 1$. For silica in the studied temperature range, we observe no such relation between D and either the mean cluster size or the mean string size and, hence, the findings for water cannot be generalized to the case of BKS silica.

An analysis of the generalized susceptibility $\chi_{ss}(\Delta t)$ revealed spatial correlations of localized, i.e. highly immobile, particles in BKS silica. On a semi-quantitative level, our results are in good agreement with that for BLJ liquids.^{24,25,26,27} More precisely, $\chi_{ss}(\Delta t)$ shows a maximum that strongly increases with decreasing T , indicating a growing length of spatial correlations between highly immobile particles. Moreover, the peak time t_4 is located in the α -relaxation regime and closely follows the temperature dependence of the structural relaxation. A quantitative comparison of the present values of χ_4^m with literature data is hampered by the different units (reduced/real) used in the simulations. However, the data for the 80:20 BLJ and 50:50 BLJ liquids again imply that the structural relaxation is more stretched for systems with pronounced SHD.

Very recently, Garrahan and Chandler^{8,9} introduced a microscopic model of supercooled liquids, which is based on three central ideas: (i) Particle mobility is sparse and

dynamics are spatially heterogeneous at times intermediate between ballistic and diffusive motion. (ii) Particle mobility is the result of dynamic facilitation, i.e., mobile particles assist their neighbors to become mobile. (iii) Mobility propagation carries a direction, the persistence length of which is larger for fragile than for strong glass formers. Our present and previous⁴⁰ results support the main ideas of the Garrahan-Chandler model on a qualitative level. Specifically, we showed that SHD exists in BKS silica and, hence, this phenomenon is not limited to non-strong model liquids. Moreover, it was demonstrated in our previous work on BKS silica⁴⁰ that dynamic facilitation is important, which is further corroborated by preliminary results for the Dzugutov liquid.⁵³ Finally, Garrahan and Chandler argue that the persistence length of the direction of mobility propagation manifests itself in the relevance of string-like motion so that the very limited importance of this type of motion for BKS silica is consistent with their idea of a shorter persistence length of particle flow direction in strong liquids.

We conclude that, at least for BKS silica, there is a subtle relation among dynamical processes on different time scales. Specifically, we suggest that the different properties of viscous liquids on the timescale of the structural relaxation are not only a consequence of quantitative differences in SHD at intermediate times, but also result from differences in the spatiotemporal propagation of mobility. Consistently, we find that the evolution of SHD at intermediate times is insensitive to the crossover in the temperature dependence of the transport coefficients, and vice versa.

Finally, we comment on the relevance of our findings with respect to real silica. The BKS model is one of the simplest models of silica, and neglects atomistic details such as three-body interactions and charge transfer processes, which are included in newer silica potentials.^{64,65} Both of these features have been demonstrated to be important for, e.g., structural transformations between silica crystal polymorphs.⁶⁵ Despite its simplicity, the BKS model reproduces many bulk dynamic and thermodynamic features of real silica. However, local dynamics involving correlated or string-like motion in the melt may well be sensitive to the re-distribution of charge during bond breakage and to higher order terms in the interaction potential. Investigation of SHD in more realistic silica models would determine this, and are underway.

V. SUMMARY

We showed that dynamics in BKS silica are spatially heterogeneous and, hence, the structural relaxation in

this model of a strong liquid cannot be described as a statistical bond-breaking process, as may have been expected from the Arrhenius-like temperature dependence of the transport coefficients. Specifically, we demonstrated that there are spatial correlations between mobile and immobile particles, respectively, the extent of which grows strongly upon cooling. In particular, the growth of dynamically correlated regions continues in the Arrhenius temperature regime. While the spatial correlations between highly mobile particles are maximum in the late- β /early- α relaxation regime of the MCT, those between highly immobile particles are biggest at later times close to the time constant of the structural relaxation. On a qualitative level, all these findings for SHD in BKS silica resemble that for non-strong model liquids. Consistently, we found that defects of the local network structure facilitate dynamics to some extent, but they are not a necessary precondition for high particle mobility. On a quantitative level, a detailed comparison with literature data showed that measures of dynamic heterogeneity at intermediate times, e.g., the mean size of clusters of mobile particles, exhibit a broad spectrum of values at the lower end of which the present results for BKS silica are found. Moreover, such comparison revealed that the α -relaxation is more nonexponential for liquids with pronounced dynamic heterogeneity at intermediate times. However, we found no evidence for a straightforward relation between the properties of dynamics on different time scales so that the correlations are subtle. In particular, the “fragile-to-strong crossover” for the transport coefficients is not accompanied by a substantial change in the temperature dependence of SHD at intermediate times. On the other hand, our results are qualitatively consistent with a microscopic model of viscous liquids put forward by Garrahan and Chandler.^{8,9} Following their ideas, we suggest that the spatiotemporal characteristics of mobility propagation play an important role in the differences between fragile and strong liquids.

Acknowledgments

We thank Y. Gebremichael and M. Bergroth for stimulating discussions. M. V. gratefully acknowledges funding by the Deutsche Forschungsgemeinschaft (DFG) through the Emmy Noether-Programm.

* Institut für Physikalische Chemie, Westfälische Wilhelms-Universität Münster, Corrensstr. 30, 48149 Münster, Ger-

many; Electronic address: mivogel@uni-muenster.de

† Electronic address: sglotzer@umich.edu

- ¹ K. Schmidt-Rohr and H. W. Spiess, Phys. Rev. Lett. 66, 3020 (1991)
- ² M. T. Cicerone, F. R. Blackburn and M. D. Ediger, Macromolecules 28, 8224 (1995)
- ³ R. Böhmer, R. V. Chamberlin, G. Diezemann, B. Geil, A. Heuer, G. Hinze, S. C. Kuebler, R. Richert, B. Schiener, H. Sillescu, H. W. Spiess, U. Tracht and M. Wilhelm, J. Non-Cryst. Solids 235-237, 1 (1998)
- ⁴ H. Sillescu, J. Non-Cryst. Solids 243, 81 (1999)
- ⁵ M. Ediger, Ann. Rev. Phys. Chem. 51, 99 (2000)
- ⁶ L. A. Deschenes and D. A. Vanden Bout, Science 292, 255 (2001)
- ⁷ G. Adam and J. H. Gibbs, J. Chem. Phys. 43, 139 (1965)
- ⁸ J. P. Garrahan and D. Chandler, Phys. Rev. Lett. 89, 035704 (2002)
- ⁹ J. P. Garrahan and D. Chandler, Proc. Nat. Acad. Soc. 100, 9710 (2003)
- ¹⁰ U. Tracht, M. Wilhelm, A. Heuer, H. Feng, K. Schmidt-Rohr and H. W. Spiess, Phys. Rev. Lett. 81, 2727 (1998)
- ¹¹ S. A. Reinsberg, X. H. Qiu, M. Wilhelm, H. W. Spiess and M. D. Ediger, J. Chem. Phys. 114, 7299 (2001)
- ¹² X. H. Qiu and M. D. Ediger, J. Phys. Chem. B 107, 459 (2003)
- ¹³ W. Götze, L. Sjogren, Rep. Prog. Phys. 55, 241 (1992)
- ¹⁴ D. N. Perera and P. Harrowell, Phys. Rev. Lett. 81, 120 (1998)
- ¹⁵ Y. Hiwatari and T. Muranaka, J. Non-Cryst. Solids 235-237, 19 (1998)
- ¹⁶ A. Onuki and R. Yamamoto, J. Non-Cryst. Solids 235-237, 34 (1998)
- ¹⁷ B. Doliwa and A. Heuer, Phys. Rev. Lett. 80, 4915 (1998)
- ¹⁸ G. Wahnström, Phys. Rev. A 44, 3752 (1991)
- ¹⁹ G. Johnson, A. I. Mel'cuk, H. Gould, W. Klein and R. D. Mountain, Phys. Rev. E 57, 5707 (1998)
- ²⁰ W. Kob, C. Donati, S. J. Plimpton, P. H. Poole and S. C. Glotzer, Phys. Rev. Lett. 79, 2827 (1997)
- ²¹ C. Donati, J. F. Douglas, W. Kob, S. J. Plimpton, P. H. Poole and S. C. Glotzer, Phys. Rev. Lett. 80, 2338 (1998)
- ²² C. Donati, S. C. Glotzer, P. H. Poole, W. Kob, S. J. Plimpton, Phys. Rev. E 60, 3107 (1999)
- ²³ C. Donati, S. C. Glotzer and P. H. Poole, Phys. Rev. Lett. 82, 5064 (1999)
- ²⁴ S. C. Glotzer, V. N. Novikov and T. B. Schröder, J. Chem. Phys. 112, 509 (2000)
- ²⁵ N. Lacevic, F. W. Starr, T. B. Schröder, V. N. Novikov and S. C. Glotzer, Phys. Rev. E 66, 030101 (2002)
- ²⁶ N. Lacevic, F. W. Starr, T. B. Schröder and S. C. Glotzer, J. Chem. Phys. 119, 7372 (2003)
- ²⁷ L. Berthier, Phys. Rev. E 69, 020201 (2004)
- ²⁸ C. Donati, S. Franz, S. C. Glotzer and G. Parisi, J. Non-Cryst. Solids 307, 215 (2002)
- ²⁹ M. Dzugutov, S. I. Simdyankin and F. H. M. Zetterling, Phys. Rev. Lett. 89, 195701 (2002)
- ³⁰ Y. Gebremichael, M. Vogel and S. C. Glotzer, J. Chem. Phys. 119, 4415 (2004)
- ³¹ Y. Gebremichael, M. Vogel and S. C. Glotzer, Molecular Simulation 30, 281 (2004)
- ³² A. Heuer and K. Okun, J. Chem. Phys. 106, 6176 (1997)
- ³³ C. Bennemann, C. Donati, J. Baschnagel and S. C. Glotzer, Nature 399, 246 (1999)
- ³⁴ Y. Gebremichael, T. B. Schröder, F. W. Starr and S. C. Glotzer, Phys. Rev. E 64, 051503 (2001)
- ³⁵ M. Aichele, Y. Gebremichael, F. W. Starr, J. Baschnagel and S. C. Glotzer, J. Chem. Phys. 119, 5290 (2003)
- ³⁶ J. Qian, R. Hentschke and A. Heuer, J. Chem. Phys. 110, 4514 (1999)
- ³⁷ N. Giovambattista, S. V. Buldyrev, F. W. Starr and H. E. Stanley, Phys. Rev. Lett. 90, 085506 (2003)
- ³⁸ S. C. Glotzer, J. Non-Cryst. Solids 274, 342 (2000)
- ³⁹ C. Dasgupta, A. V. Indrani, S. Ramaswamy and M. K. Phani, Europhys. Lett. 15, 307 (1991)
- ⁴⁰ M. Vogel and S. C. Glotzer, Phys. Rev. Lett. (in press); cond-mat/0402427
- ⁴¹ C. A. Angell, J. Non-Cryst. Solids 131-133, 13 (1991)
- ⁴² B. W. H. van Beest, G. J. Kramer, R. A. van Santen, Phys. Rev. Lett. 64, 1955 (1990)
- ⁴³ J.-L. Barrat, J. Badro and P. Gillet, Molecular Simulation 20, 17 (1997)
- ⁴⁴ J. Horbach and W. Kob, Phys. Rev. B 60, 3169 (1999)
- ⁴⁵ J. Horbach and W. Kob, Phys. Rev. E 64, 041503 (2001)
- ⁴⁶ W. Kob, J. Phys.: Condens. Matter 11, R85 (1999)
- ⁴⁷ K. Binder, J. Non-Cryst. Solids 274, 332 (2000)
- ⁴⁸ I. Saika-Volvod, P. H. Poole and F. Sciortino, Nature 412, 514 (2001)
- ⁴⁹ K. Vollmayr, W. Kob and K. Binder, Phys. Rev. B 54, 15808 (1996)
- ⁵⁰ J. Horbach, W. Kob, K. Binder and C. A. Angell, Phys. Rev. E 54, 5897 (1996)
- ⁵¹ J. Horbach, W. Kob and K. Binder, Eur. Phys. J. B 19, 531 (2001)
- ⁵² K.-U. Hess, D. B. Dingwell and E. Rössler, Chem. Geol. 128, 155 (1996); E. Rössler, K.-U. Hess and V. N. Novikov, J. Non-Cryst. Solids 223, 207 (1998)
- ⁵³ M. Bergroth, M. Vogel and S. C. Glotzer (unpublished results)
- ⁵⁴ M. P. Allen and D. J. Tildesley, *Computer Simulation of Liquids* (Oxford University Press, New York, 1990)
- ⁵⁵ J. C. Mikkelsen, Appl. Phys. Lett. 45, 1187 (1984)
- ⁵⁶ G. Brebec, R. Seguin, C. Sella, J. Bevenot, J. C. Martin, Acta Metall. 28, 327 (1980)
- ⁵⁷ F. W. Starr, F. Sciortino and H. E. Stanley, Phys. Rev. E 60, 6757 (1999)
- ⁵⁸ S. Sastry, Nature 409, 164 (2001)
- ⁵⁹ A. Scala, F. W. Starr, E. La Nave, F. Sciortino and H. E. Stanley, Nature 406, 166 (2000)
- ⁶⁰ Y. Gebremichael, PhD thesis, University of Maryland, USA (2004); Y. Gebremichael, M. Vogel, F. W. Starr and S. C. Glotzer (in preparation)
- ⁶¹ T. B. Schröder, S. Sastry, J. C. Dyre and S. C. Glotzer, J. Chem. Phys. 112, 9834 (2000); T. B. Schröder, cond-mat/0005127
- ⁶² C. Bennemann, W. Paul, K. Binder and B. Dünweg, Phys. Rev. E 57, 843 (1998)
- ⁶³ F. W. Starr, S. Harrington, F. Sciortino and H. E. Stanley, Phys. Rev. Lett. 82, 3629 (1999)
- ⁶⁴ L. Duffrene and J. Kieffer, J. Phys. and Chem. of Solids 59, 1025 (1998)
- ⁶⁵ L. Huang and J. Kieffer, J. Chem. Phys. 118, 1487 (2003)